International Journal of Mass Spectrometry 188 (1999) 205–212

A mass spectrometric study on the formation of ionic Ta-containing oxides from laser ablation of Ta and Ta_2O_5 in O_2 ambient

Xuefeng Wang, Zhenning Gu, Qizong Qin*

Laser Chemistry Institute, Fudan University, Shanghai 200433, People's Republic of China

Received 7 December 1998; accepted 18 February 1999

Abstract

Formation of the ionic Ta-containing oxides in 532 nm laser ablation of Ta and Ta_2O_5 in an ambient O_2 is investigated using a time-of-flight mass spectrometry. Mass spectra are taken both in vacuum and in an oxygen ambient. Results of the detected positive charged species show that besides the TaO^+ and TaO_2^+ ions, the new species such as $(O_2)TaO^+$ and $(O_2)Ta(O_2)^+$ are observed for the first time. The molecular geometries of the Ta-containing ionic oxides are predicted. Along with the theoretically calculated energy changes of possible oxidation reactions involved, the reaction channels for the formation of the ionic Ta-containing oxides are discussed. (Int J Mass Spectrom 188 (1999) 205–212) © 1999 Elsevier Science B.V.

Keywords: Laser ablation; Time-of-flight mass spectrometry; Ta-containing ionic oxides

---

1. Introduction

Pulsed laser deposition (PLD) has been widely used in the deposition of various metal oxides films [1]. Recently, there have been many reports about Ta_2O_5 thin films fabricated by PLD by using Ta_2O_5 or metallic Ta as a target [2–4]. It has been proven that the oxygen content in such films affects their qualities notably [5,6], so an oxygen ambient is always needed during the PLD process to avoid the growth of oxygen deficient films. The oxygen pressure and the target–substrate distance were found to be the two important parameters that influence both the structure and the composition of the films [7–10]. It means that the reactions of the ablated species with ambient oxygen molecules in the PLD are of crucial importance for the Ta_2O_5 thin film growth.

The optical emission spectroscopy [4] and angle-resolved quadrupole mass spectrometry [11] have been used in our group to examine the composition and evolution of the plasma produced by the pulsed laser ablation of Ta and Ta_2O_5, and to understand the tremendous role of ambient oxygen in the laser ablation process. It is known that the time-of-flight mass spectrometry (TOF-MS) has usually been employed in the diagnostics of ablation process. The particular advantages of TOF-MS are its high collection efficiency of the ablated ions and its capability of recording a complete mass spectrum at each laser shot as well as providing in situ diagnostics of the interaction between the ionic species and ambient molecules [12]. The TOF-MS techniques have been suc-

---

* Corresponding author. E-mail: qzqin@srcap.sth.sh.cn

PII S1387-3806(99)00034-2

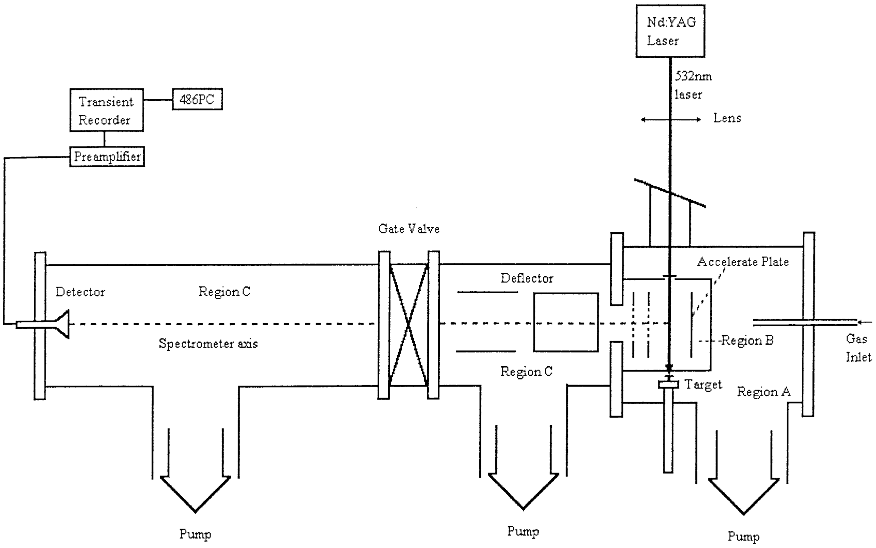

Fig. 1. Schematic diagram of time-of-flight mass spectrometer.

cessfully employed by many laboratories [12,13] to investigate the evolution of the plume composition and the formation of the charged species in the laser ablation of $Pb(Ti_{0.48}Zr_{0.52})O_3$ (PZT) and $YBa_2Cu_3O_{7-\delta}$ (YBCO) targets. However, there is no report on the characterization of the charged species in the laser ablation of Ta_2O_5/Ta by using a TOF-MS technique.

The motivation of this work is to get insight into the formation of ionic Ta-containing oxides in 532 nm laser ablation of a Ta or Ta_2O_5 target in an ambient oxygen. The relative intensities of the Ta-containing positive ions are measured as a function of the oxygen pressure and the probe distance from the target surface. Possible pathways for the formation of these positive ions are proposed by theoretical consideration and the experimental results.

2. Experimental and theoretical procedures

2.1. Time-of-flight mass spectrometric measurements of laser ablation of Ta/Ta_2O_5

The apparatus used in the present experiment is shown in Fig. 1. The reaction chamber (region A) was evacuated to a base pressure of 10^{-3} Pa using an oil diffusion pump and equipped with a rotating target holder. An oxygen gas was introduced into the chamber and its pressure was adjusted with a leak valve. The 532 nm laser beam was provided by the second harmonic of a *Q*-switched Nd:YAG laser (Quanta Ray DCR-2), and focused onto the target with a 1-mm-diameter spot. The laser beam irradiated on a metallic Ta or a Ta_2O_5 (99.99%) pellet target along the target surface normal. The repetition rate of the pulsed laser was 20 Hz with a pulse width of 8 ns. The laser intensity was measured by a pyroelectric power meter.

The ablated species entered the ion accelerate chamber through a 5-mm-diameter aperture and reached the extraction region B with a base pressure of 10^{-4} Pa. The charged species were extracted perpendicularly along the target surface normal and accelerated by a pulsed electric field (1800 V) with a risetime of 0.2 μs and a pulse duration adjustable in the range 1–4 μs. The accelerated ions flew through a deflector, and then entered a 120 cm field-free drift tube (region C), which was differentially pumped with two turbomolecular pumps. The ions were detected by a dual microchannel plate (MCP). The signals from the MCP detector were amplified by a pre-amp (EG&G ORTEC, 9305) and then fed into a

100 MHz transient recorder interfaced to a 486 PC computer. Each TOF mass spectrum was obtained by averaging over 100 laser shots.

For spatially resolved measurements, the target can be moved in order to vary the probe distance *d* between target surface and the flight tube axis. Generally, the plume range L_p is defined as the distance from the target surface where the internal pressure is equal to the ambient gas environment [13]. In our experiment, the observation region of the TOF-MS was set at relatively long distance (>55 mm) to avoid the influence of the ablated species in the excited state. This feature allowed us to examine the transport and gas phase reactions of the ablated ionic species with ambient O_2 molecules, and to analyze the evolution of ionic species in ablated plume as a function of the probe distance from the target surface.

2.2. Theoretical calculations

The theoretical calculations were performed to provide the geometric parameters, structure features of the observed ionic Ta-containing oxides and energy changes for their formation. Geometries of Ta-containing ionic oxides were optimized at the second order Møller–Plesset (MP2) level to find the globe minima using GAUSSIAN 94 package of computer codes [14]. The D95 basis set was employed for oxygen atoms and LanL2DZ basis set with an Ar-like effective core potential [15–17] was used for Ta. Generally, the Ta atom basis sets were described with explicit seven- and three-electron valence shells respectively, with the chemically less active core electrons pictured with effective potential. Fundamental frequencies were obtained with the calculated complete quadratic force constant matrices at the optimized structure.

3. Results

3.1. Ablation of metallic Ta in O_2 ambient

Fig. 2(a) shows the TOF mass spectra of ions produced by ablation of metal Ta in an ambient O_2 at different pressure. It can be seen that only one Ta^+ peak appears at low O_2 pressure. TaO^+ and TaO_2^+ are produced in succession as O_2 pressure increased, but there are no further Ta-containing ionic oxides being observed even when O_2 pressure was increased up to 5.3 Pa. The dependence of the intensities of Ta^+, TaO^+, and TaO_2^+ on the ambient oxygen pressure is presented in Fig. 2(b). Variation appearing in Fig. 2(b) provides a clear sight into the oxidation processes of the ablated Ta-containing species with O_2 as we will discuss later.

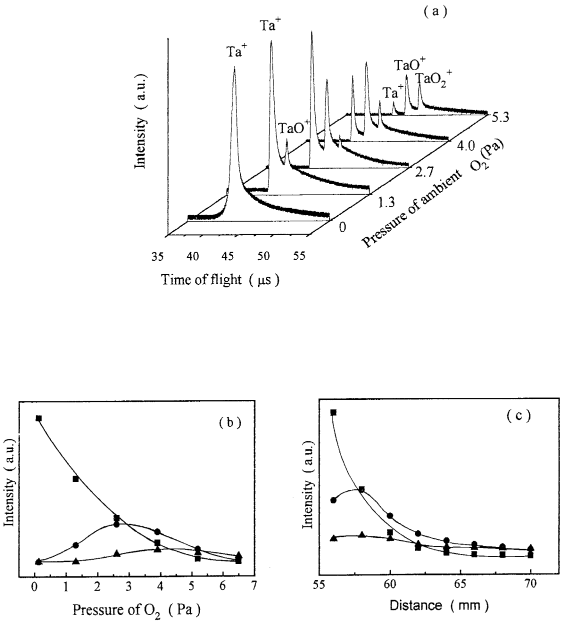

Fig. 2. Intensity variations of Ta-containing ions from ablation of metallic Ta, closed square: Ta^+, closed circle: TaO^+, closed triangle: TaO_2^+. (a) TOF-MS of ions at different ambient O_2 pressure. (b) Influence of ambient O_2 pressure on intensities of ablated ions. (c) Spatial distribution of ablated ions (P_{O_2}: 4 Pa).

Spatial distributions of Ta-containing positive ionic species are observed by measuring the signal intensities of each detected ions as a function of the probe distance *d* at definite O_2 pressure. As shown in Fig. 2(c), the majority of Ta-containing ions are distributed in the region of $d \leq 60$ mm. Out of that range, most ions are probably neutralized with electrons or with negatively charged ions. Moreover, the decreasing rate of Ta^+ intensity with *d* is prominent, suggesting that besides neutralization process, oxidation reactions of Ta^+ ions with O_2 ambient takes place and Ta^+ ions convert to TaO^+ and TaO_2^+.

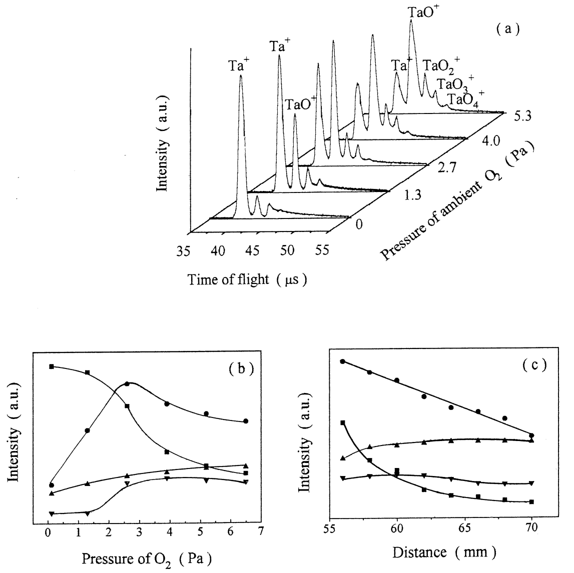

Fig. 3. Intensity variations of Ta-containing ions from ablation of Ta_2O_5, closed square: Ta^+, closed circle: TaO^+, closed triangle: TaO_2^+, closed inverted triangle: TaO_3^+. (a) TOF-MS of ions at different ambient O_2 pressure. (b) Influence of ambient O_2 pressure on intensities of ablated ions. (c) Spatial distribution of ablated ions (P_{O_2}: 6 Pa).

3.2. Ablation of Ta_2O_5 in O_2 ambient

TOF mass spectra measured at various pressures of ambient oxygen in the ablation of a Ta_2O_5 pellet instead of Ta as a target are shown in Fig. 3(a). It can been seen that the Ta^+ ion is a major product, and TaO^+ and TaO_2^+ ions are also observed under vacuum condition. As the pressure of ambient O_2 was increased, the intensity of TaO^+ increased and Ta^+ obviously decreased. The new Ta-containing oxides $(O_2)TaO^+$ and $(O_2)Ta(O_2)^+$ with *m*/*e* 129 and 145, respectively, were observed for the first time. Intensities of Ta^+, TaO^+, TaO_2^+, and $(O_2)TaO^+$ ions as a function of ambient O_2 pressure are shown in Fig. 3(b). Based on analyzing the trends of intensities of each ion with ambient O_2 pressure, it is evident that the oxidation reactions also take place between Ta-containing species and O_2.

Spatial distribution of ionic species from ablation of Ta_2O_5 in oxygen ambient is shown in Fig. 3(c). It can be seen that the intensity of Ta^+ ion dropped rapidly and the intensity of TaO^+ ion decreased linearly with increasing probe distance *d*. But the intensity of TaO_2^+ ion increased slightly at first then remained unchange at $d \geq 60$ mm. Since the measured intensities of $(O_2)TaO^+$ were very low, their intensity variation was less obvious compared with the other Ta-containing ions.

The calculated geometry parameters and the vibrational frequencies are listed in Table 1. The predicted structures of TaO^+, TaO_2^+, $(O_2)TaO^+$, and $(O_2)Ta(O_2)^+$ ions are presented in Fig. 4. The theoretically calculated energy changes of possible reactions between ablated ground-state tantalum-containing ions and molecular O_2 or atomic O are listed in Table 2 and discussed in the next section.

4. Discussion

Our previous study on the laser ablation of metallic Ta showed that when metallic Ta is used as target, only atomic Ta and ionic Ta^+ could be observed as the ablated species under vacuum condition. By using Ta_2O_5 instead of Ta as a target, a copious amount of ions and neutral ablated species, such as atomic O, Ta, ionic O^+, Ta^+, TaO^+, and TaO_2^+ as well as molecular O_2, TaO, and TaO_2 were detected by quadrupole mass spectrometry [18]. In addition, our spatial emission spectroscopic study on 532 nm laser ablation of Ta_2O_5 in ambient O_2 suggested that the interactions of the ablated species with ambient O_2 are quite complicated. So, it is important to examine the oxidation reactions of ionic Ta-containing ablated species with ambient oxygen molecules in the laser ablated plume using a time-of-flight mass spectrometric technique.

Based on our experimental data as well as theoretical calculated results in Tables 1 and 2, the formation channels of the positive ionic Ta-containing products are discussed as follows.

4.1. Channels for TaO^+ formation

During laser ablation of metallic Ta in ambient oxygen, large amounts of Ta atoms are generated from the target surface and ionized by electron impact ionization within the laser induced plasma plume.

Table 1
Calculated geometries and frequencies of the TaO^+, TaO_2^+, TaO_3^+, and TaO_4^+ molecules

Species	Calculated geometries (R/Å): bond length, (A/deg): bond angle, (D/deg): dihedral angle	Calculated frequencies (ν/cm^{-1})
TaO^+	R(Ta–O) = 1.742	909.0
TaO_2^+	$R(Ta^2–O^1) = R(Ta^2–O^3) = 1.778$ $A(123) = 101.7$	946.1, 886.8, 346.7
$(O_2)TaO^+$	$R(Ta^2–O^1) = 1.783$ $R(Ta^2–O^3) = R(Ta^2–O^4) = 1.949$ $R(O^3–O^4) = 1.647$ $A(123) = 104.3, A(124) = 104.2$ $A(324) = 50.0, D(4213) = 51.7$	834.9, 822.5, 693.0, 577.0, 260.4, 196.4
$(O_2)Ta(O_2)^+$	$R(Ta^2–O^1) = R(Ta^2–O^5) = 1.959$ $R(Ta^2–O^3) = R(Ta^2–O^4) = 1.925$ $R(O^1–O^3) = R(O^3–O^5) = 1.637$ $A(123) = A(425) = 103.2$ $A(124) = A(325) = 49.8$ $A(324) = 102.1, A(125) = 141.3$ $D(4213) = 94.8, D(5213) = 40.0$ $D(5214) = -54.9, D(5234) = -97.1$	847.7, 842.1, 732.8, 647.2, 616.2, 591.3, 257.4, 180.5, 60.2

Then the ionic Ta^+ species are oxidized by ambient oxygen molecules to form TaO^+ by

$$Ta^+(^5F) + O_2(^3\Sigma) \rightarrow TaO^+(^1\Sigma) + O(^3P),$$
$$\Delta E = -72.67 \text{ kcal mol}^{-1} \quad (1)$$

Since the atomic O can be produced from dissociation of O_2 in the plasma and from reaction (1), it makes the following reaction:

$$Ta^+(^5F) + O(^3P) \rightarrow TaO^+(^1\Sigma),$$
$$\Delta E = -160.06 \text{ kcal mol}^{-1} \quad (2)$$

possible, which also forms TaO^+.

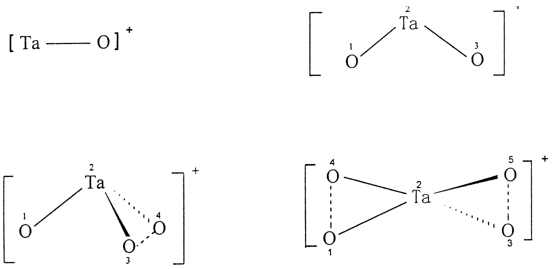

Fig. 4. The predicted structures of Ta-containing ionic oxides (refer to Table 1 for detailed structural parameters).

Our theoretical calculation results indicates that reaction (2) is exothermic with a rather negative energy change, and the activation energy of such an ion–atom reaction is considerably low.

When laser ablation of Ta_2O_5 target occurred under vacuum condition, TaO^+ ion was observed as a major ablated product in the TOF mass spectrum [see Fig. 3(a)]. Our previous report [18] showed that there were quite a few O atoms and almost no O_2 molecules produced from the target surface in this case. Thus, the occurrence of TaO^+ could be due to reaction (2) taking place in the ablated plume. As laser ablation of Ta_2O_5 occurred in an O_2 ambient, intensity of TaO^+ ions enhanced dramatically with the increasing of oxygen pressure accompanying the expense of Ta^+. These results imply that both exothermic reactions (1) and (2) occurred. Meanwhile, the ablated plume was surrounded by ambient O_2, the amount of molecular oxygen around was much more than that of atomic O. Therefore, reaction (1) might be the dominant channel for the formation of TaO^+. We neglect the possibility of formation of TaO^+ from reaction of atomic Ta with O^+ since the O^+ ion signal was absent in our mass spectra.

Table 2
Energy changes of possible reaction channels for the formation of tantalum-containing ions

Reaction	Possible reaction channel	Calculated energy change ΔE (kcal mol^{-1})
(1)	$Ta^+(^5F) + O_2(^3\Sigma) \rightarrow TaO^+(^1\Sigma) + O(^3P)$	-72.67
(2)	$Ta^+(^5F) + O(^3P) \rightarrow TaO^+(^1\Sigma)$	-160.06
(3)	$Ta^+(^5F) + O_2(^3\Sigma) \rightarrow TaO_2^+(^1\Sigma)$	-254.89
(4)	$TaO^+(^1\Sigma) + O_2(^3\Sigma) \rightarrow TaO_2^+(^1\Sigma) + O(^3P)$	-94.83
(5)	$TaO^+(^1\Sigma) + O_2(^3\Sigma) \rightarrow (O_2)TaO^+(^1\Sigma)$	-119.43
(6)	$TaO_2^+(^1\Sigma) + O_2(^3\Sigma) \rightarrow (O_2)TaO^+(^1\Sigma) + O(^3P)$	$+62.79$
(7)	$TaO_2^+(^1\Sigma) + O_2(^3\Sigma) \rightarrow (O_2)Ta(O_2)^+(^1\Sigma)$	$+54.19$
(8)	$TaO_3^+(^1\Sigma) + O(^3\Sigma) \rightarrow (O_2)Ta(O_2)^+(^1\Sigma)$	-8.60

As shown in Fig. 3(b), the intensity of TaO^+ ions increased sharply with the increasing of oxygen pressure and declined afterwards. This result implies that TaO^+ ions are produced rapidly via reactions (1) and (2) when more oxygen molecules are available in an O_2 ambient. The decrease of TaO^+ intensity at higher O_2 pressure suggests that a number of secondary reactions [such as exothermic reactions (4), (5), and (6)] (see Table 2) might occur which expend TaO^+ ions.

Spatial distributions of TaO^+ ions shown in Figs. 2(c) and 3(c) indicate that the oxidation processes happened more frequently in the range relatively near the target. As the probe distance increased, the intensity of TaO^+ became less. This is probably because more TaO^+ ions are neutralized by colliding with electrons as the ablated plume evolved a longer distance.

4.2. Channels for TaO_2^+ formation

As shown in Fig. 2(a), TaO_2^+ ions appeared during laser ablation of metallic Ta in an O_2 ambient when O_2 pressure increased beyond 2.5 Pa. Since Ta^+ ion is the major ablated product in this case, TaO_2^+ ions are expected to be formed by adduction

$$Ta^+(^5F) + O_2(^3\Sigma) \rightarrow TaO_2^+(^1\Sigma),$$
$$\Delta E = -254.89 \text{ kcal mol}^{-1} \qquad (3)$$

In addition, reaction of TaO^+ with O_2 via

$$TaO^+(^1\Sigma) + O_2(^3\Sigma) \rightarrow TaO_2^+(^1\Sigma) + O(^3P),$$
$$\Delta E = -94.83 \text{ kcal mol}^{-1} \qquad (4)$$

which is expected to be exothermic, could also take place to form TaO_2^+ ion.

Viewing merely from the exothermicity of reaction (3), it seems that TaO_2^+ could be formed more easily than TaO^+ in ambient oxygen. But our experimental results indicate the reverse trend [see Fig. 2(a)]. This infers that despite the high exothermicity of reaction (3), its activation energy might be somewhat high, which leads to the less intensity of TaO_2^+.

In the case of laser ablation of Ta_2O_5 in vacuum, TaO_2^+ ion was also observed in Fig. 3(a). It might be ejected directly from the Ta_2O_5 target. When laser ablation of Ta_2O_5 target occurred in an O_2 ambient, increasing TaO_2^+ intensity with an increase of oxygen pressure shown in Fig. 3(b) reveals that besides directly ejected from the target, TaO_2^+ could also be formed from Ta^+ and TaO^+ reacting with oxygen via reactions (3) and (4). Similarly, the possible formation channel of TaO_2^+ from reaction of TaO with ionic O^+ is not considered because of the absence of O^+ in our experiment.

4.3. Channels for $(O_2)TaO^+$ formation

From the measured TOF-MS as shown in Fig. 3(a), the signal peak at *m/e* 129 can be attributed to "TaO_3^+." However, the highest oxidation valence of Ta atom is +5, it means that the formation of TaO_3^+

is unreasonable. The calculated geometry of TaO_3^+ (shown in Fig. 4) shows that the bond length of the three Ta–O bonds are not equal. One bond is somewhat shorter (1.782 Å) than the other two (1.949 Å). The two oxygen atoms at the ends of the longer Ta–O bonds are much nearer from each other (1.647 Å). Thus the ablated species with m/e 129 might be $(O_2)TaO^+$, a complex ion of TaO^+ with O_2. From the calculated energy changes of reactions (5) and (6) listed in Table 2, it is reasonable to consider the exothermic reaction of TaO^+ with O_2 to be the major formation channels of $(O_2)TaO^+$.

A remarkable fact in our experiment is that the $(O_2)TaO^+$ ions were formed only in ablation of Ta_2O_5 but not in ablation of metallic Ta. Possible formation channel of $(O_2)TaO^+$ ion via reaction (5) includes TaO^+ ion as a reactant. The difference between these two ablation cases is that TaO^+ ions in ablation of metallic Ta completely come from the oxidation of Ta^+ by oxygen, whereas part of TaO^+ ions in the Ta_2O_5 ablation are ejected directly from Ta_2O_5 target. It seemed that only those directly ejected TaO^+ ions are able to undergo reaction (5). The low intensity of $(O_2)TaO^+$ ion observed in TOF mass spectra might be due to the low concentration of the directly ejected TaO^+ ions from Ta_2O_5 target.

4.4. Channels of $(O_2)Ta(O_2)^+$ formation

Based on our theoretical calculated result listed in Table 1, the most reasonable geometric structure of the observed "TaO_4^+" ($m/e = 145$) should be $(O_2)Ta(O_2)^+$. The O atoms link the Ta^+ by weak bonds with bond length of 1.925 and 1.959 Å, respectively, which are much longer than the distance between the end pairs of O atoms (1.637 Å). It seems that due to bonding with Ta^+, the O–O bonds were stretched and weakened compared with the bond of the O_2 molecule.

The $(O_2)Ta(O_2)^+$ ion was observed only in ablation of Ta_2O_5 shown in Fig. 3(a). The possible formation channel of $(O_2)Ta(O_2)^+$ via reaction (7) (see Table 2) is endothermic. However, the TaO_2^+ ion in the plume can be effective in surmounting the substantial energy barrier and promote the formation of $(O_2)Ta(O_2)^+$ ion by combining an O_2 molecule. So reaction (7) could be the major channel as inferred from the calculated structure of $(O_2)Ta(O_2)^+$. Calculated energy change showed that $(O_2)Ta(O_2)^+$ ion could also be formed exothermically from $(O_2)TaO^+$ ion with atomic oxygen [via reaction (8) shown in Table 2]. However, it could not be the dominant channel because of the much smaller amount of O atoms compared with large amount of O_2 around. Besides, the energy change of reaction (7), indicates that $(O_2)Ta(O_2)^+$ ions are much more possible to dissociate rather than form. This could explain why $(O_2)Ta(O_2)^+$ ions appeared with such a small signal in the TOF mass spectra.

5. Conclusion

The oxidation of the ground-state tantalum-containing ions from laser ablation of Ta and Ta_2O_5 in ambient O_2 has been studied by time-of-flight mass spectrometry. The atomic Ta^+ ions and oxide ions TaO^+, TaO_2^+, $(O_2)TaO^+$, and $(O_2)Ta(O_2)^+$ are observed. Analysis of their TOF mass spectra reveals that Ta^+ ions from ablation of Ta could be oxidized to TaO^+ and TaO_2^+ by ambient oxygen, and TaO^+ and TaO_2^+ ions from ablation of Ta_2O_5 could combine O_2 to produce $(O_2)TaO^+$ and $(O_2)Ta(O_2)^+$, respectively. The theoretical calculations of molecular geometries of the ionic oxides as well as the energy changes of possible ground-state reactions involving Ta-containing ions are performed to predict the possible formation channels of the Ta-containing ionic oxides.

Acknowledgements

This work was supported by the National Natural Science Foundation of China (grant no. 29683001).

References

[1] D.B. Chrisey, J.S. Hovwitz, P.C. Dorsey, J.M. Pond, Laser Focus World, May (1995) 115.
[2] N. Inoue et al., Appl. Surf. Sci. 96 (1996) 656.

[3] M.F. Zhou, Z.W. Fu, Q.Z. Qin, Appl. Surf. Sci. 108 (1997) 399.

[4] Z.W. Fu, M.F. Zhou, Q.Z. Qin, Appl. Phys. A. 65 (1997) 445.

[5] K. Fukushimura et al., J. Appl. Phys. 77 (1995) 5406.

[6] U. Gambardella et al., Appl. Surf. Sci. 86 (1995) 45.

[7] A. Inam et al., Appl. Phys. Lett. 53 (1988) 908.

[8] X.D. Wu et al., Appl. Phys. Lett. 58 (1991) 304.

[9] R.E. Muenchausen et al., Appl. Phys. Lett. 56 (1990) 578.

[10] A. Morimoto et al., Mater. Res. Soc. Symp. Proc. 191 (1990) 31.

[11] Z.H. Han, J.J. Lu, H.J. Dang, Z.G. Dai, Q.Z. Qin, Acta Phys. Chem. Sin. 13 (1997) 140.

[12] S. Amoruso et al., Appl. Phys. A. 62 (1996) 533.

[13] V. Berardi et al., J. Appl. Phys. 76 (1994) 8077.

[14] M.J. Frisch, G.W. Trucks, H.B. Schlegel, P.M.W. Gill, B.G. Jonhnson, M.A. Robb, J.R. Cheeseman, T.A. Keith, G.A. Petersson, J.A. Montgomery, K. Raghavachari, M.A. Al-Laham, V.G. Zakrzewski, J.V. Ortiz, J.B. Foresman, J. Cioslowski, B.B. Stefanov, A. Nanayakkara, M. Challacombe, C.Y. Peng, P.Y. Ayala, W. Chen, M.W. Wong, J.L. Andres, E.S. Replogle, R. Gomperts, R.L. Martin, D.J. Fox, J.S. Binkley, D.J. Defrees, J. Baker, J.P. Stewart, M. Head-Gordon, C. Gonzalez, and J.A. Pople GAUSSIAN 94 (Revision B2), Gaussian Inc., Pittsburgh, PA, 1995.

[15] P.J. Hay, W.R. Wadt, J. Chem. Phys. 82 (1985) 270.

[16] W.R. Wadt, P.J. Hay, J. Chem. Phys. 82 (1985) 184.

[17] P.J. Hay, W.R. Wadt, J. Chem. Phys. 82 (1985) 299.

[18] Q.Z. Qin, Z.H. Han, H.J. Dang, J. Appl. Phys. 83 (1998) 6082.